Water-ice clouds in the LMDs Martian General Circulation Model

F. Montmessin, **F. Forget,** *Laboratoire de Météorologie Dynamique (LMD) de Jussieu, Paris, France (montmes@aero.jussieu.fr)*

Introduction:

The interest for Martian water ice clouds has recently taken a new extent given their likely involvement both in climate and in the hydrological cycle (Clancy et al., 1996). Previous related microphysical studies have already discussed the complex interactions between airborne dust and clouds (Michelangeli et al., 1993). Whereas water ice mantles upon dust cores enhance sedimentation rates and thus possibly change the vertical distribution of dust and water, the advection of clouds by winds could also modulate the geographical distribution of volatiles. Within this context, only 3D modeling based on the use of Martian General Circulation Models (MGCM) is able to give us a consistent clue of the global climatic aspects of Martian clouds.

Alike their terrestrial counterparts, Martian clouds feature patchy structures that can not be easily caught by the coarse spatial resolution of GCMs. On the other hand, the major manifestations of Martian nebulosity, such as the "aphelion cloud belt" (Clancy et al., 1996) or the "polar hoods" (Christensen et Zurek, 1984), evolve on horizontal scales that are suitable to a GCM representation.

The study presented here is part of a project conducted with the MGCM developed in a French laboratory (LMD). Our final objective is to dispose of a model capable of simulating Martian climate while accounting for the radiative feedback of water ice clouds. The current stage of development does not allow us to treat the effects of clouds on the radiative budget. However, we have implemented a simplified cloud scheme enabling the prediction of nebulosity as a function of space and time.

The purpose of this paper is motivated by the will to highlight the considerable role of clouds as a mobile reservoir for water. Even though Richardson and Wilson (2002a) have already shown the sensitivity of the hydrological cycle to the microphysical properties of water ice crystals, we would like to give this effect a more quantitative assessment through a comparison of two cloud schemes differing by their conceptual assumptions. Each of these models, along with their respective results, will be compared to observational data. Their mutual differences will be discussed in order to grasp the net effect of clouds on the geographical distribution of water on Mars.

Model description:

"Core" component. The LMDs MGCM is a grid point dynamic model developed to study meteorological phenomena of the Martian atmosphere. A complete description of both the dynamical and physical parts of the model is given in Forget et al. (1999). One novel aspect of this model has been achieved owing to the recent soundings of the TES spectrometer. Indeed, the geographical distribution of dust –the unique input of the radiation code– has been adjusted in order to satisfy a large set of observed temperature profiles. This *ad hoc* prescription of dust guarantees a consistent background to study species like clouds which are extremely sensitive to their thermal environment. In the following, we will mostly emphasize the specific routines used to represent the physical processes affecting water vapor and ice. All the results presented throughout this paper have been obtained using a spatial resolution of 48x32x25; i.e. 48 longitudinal points-32 latitudinal points and 25 points irregularly spread on the vertical axis.

Volatile transport. Since variations with space and time of the dust quantity are prescribed, only water vapor and ice are physically transported in the model. The MGCM dynamical core includes a built-in advection scheme (based on a Van-Leer formulation) used to solve the transport of tracers by the model resolved winds. In addition, each phase of water is vertically redistributed in a way depending on the turbulent kinetic energy diagnosed by the model in each grid box. This additional transport, akin to a diffusion process, is commonly employed to simulate "eddy mixing". This method is also applied to compute water fluxes between surface and air wherever a ground layer of ice is susceptible of subliming.

Sources and sinks. In a future version of the model, regolith adsorption will be accounted for together with our cloud scheme. This task is currently undergone and is presented elsewhere (see H. Boettger et al., this issue) but is not included in this version. As a consequence, the unique ground source of water is prescribed north of 80°N where the water ice permanent cap (called NPC in the remainder of the paper) has been identified. A "thick" dry ice deposit is set south of 85°S in order to simulate cold trapping by the CO_2 residual cap.

Microphysical processes. The first cloud scheme (***basic cloud model***) does not allow water ice to be transported neither vertically nor horizontally; atmospheric water ice is not even considered as a tracer. This cloud scheme follows the one described by Haberle and Jakosky (1990); i.e. whenever relative humidity in a grid box is larger than 100%, the excess is instantaneously transferred to the next lowest layer. This process is continuously repeated all

over the atmospheric column and can ultimately lead to water ice deposition on the surface.

The second, "reference", cloud scheme (***evolution 1 scheme***) adopts parametrizations fulfilling most of the elementary requirements of microphysics. As mentioned previously, we do not consider dust as a "physical" quantity: we therefore make abstraction of dust-cloud interactions. Whereas such a physical coupling likely influences cloud evolution, its estimation suffers a lack of experimental data (for instance, the efficiency of nucleation on dust grains remains poorly constrained). In order to keep a somewhat realistic approach, we specify a number of condensation nuclei N in each grid box as a function of latitude and time used as an input to our microphysics scheme in order to compute the mean radius of ice crystals in a grid box. Our method employs a first order moment determination of cloud properties since only one three dimensional field is allocated to water ice, namely its mass mixing ratio M. The variation of M during a time step is computed while considering processes of condensational growth, gravitational settling and transport.

In both models, we have included the ability of water ice deposits to modify surface properties. Consequently, the local surface albedo is set to a value of 0.4 wherever an ice layer thicker than 5 µm is predicted by the model. This value appears reasonable as regards to the work of Bass and Paige (2000).

Simulation results:

Driving mechanisms of the Martian water cycle have been deeply studied and progressively reveal their nature (e.g. Houben et al. [1997], Richardson and Wilson [2002b]). For this reason, we will only focus on the specific question of cloudiness, assuming that salient features of the water cycle are already known by the reader.

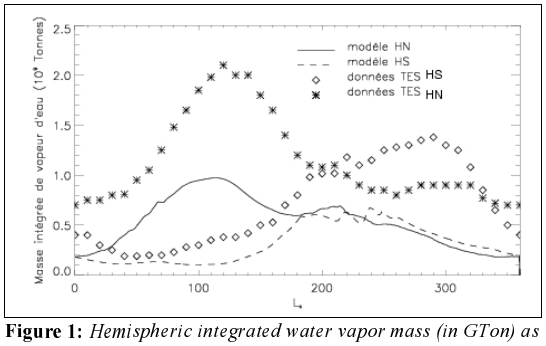

Figure 1: *Hemispheric integrated water vapor mass (in GTon) as a function of solar longitude (HN: northern hemisphere, HS: southern hemisphere). Simulated evolution of humidity (bold and dashed curves) can be compared to TES data (stars and circles).*

Basic cloud model. About eight years of simulation are required to reach a steady state; i.e. interannual fluctuations do not exceed 1%. As suggested by Jakosky (1983), such a spin-up timescale is necessary for dynamical processes to set up a latitudinal gradient in response to polar water abundances (which are forced by local thermodynamical conditions). We use water vapor abundances derived by the TES spectrometer to evaluate the consistency of the model predictions. Figure 1 displays the modeled and observed seasonal evolution of atmospheric water vapor in both hemispheres.

Despite an overall good match of seasonal tendencies, the model fails at predicting the correct abundances of water vapor, having values that are a factor of two or three lower than observed.

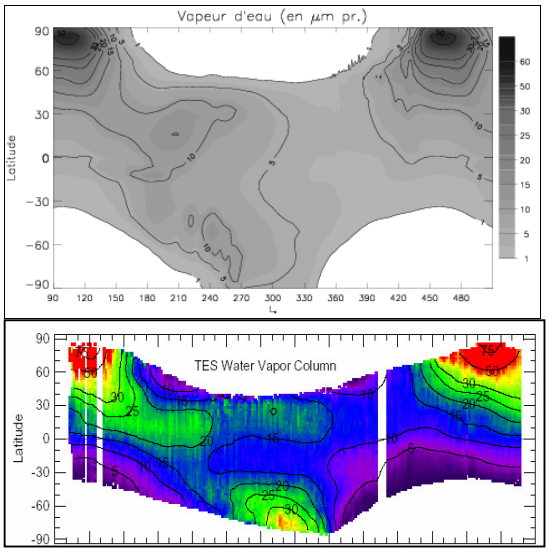

Figure 2: *Seasonal and latitudinal distribution of water vapor abundances (in pr.. µm)*-**Upper graph***: as predicted by the model*-**Lower graph***: as derived from TES soundings (Smith, 2002).*

This discrepancy is further supported by figure 2 which clearly indicates a lack of humidity, mostly in the mid-latitudes regions. This statement clearly motivates the higher level of sophistication provided by our "reference" cloud scheme which results are presented below.

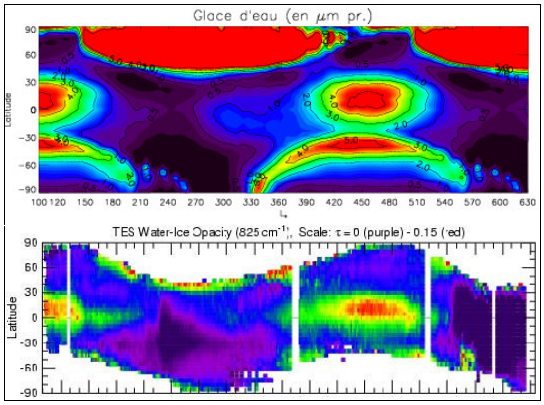

Figure 3: *Seasonal and latitudinal distribution of water ice abundances* **Upper graph***: as predicted by the model (in pr.. µm)*--**Lower graph***: as derived from TES soundings (Smith, 2002).*

Evolution 1 scheme. Before discussing the relative differences between the results of the two models, we

first compare the distribution of clouds predicted by this cloud scheme to the TES data (Figure 3). This figure only permits to assess the qualitative consistency of our predictions since modeled water ice abundances have to be compared to observed cloud opacities. The orbital variation clearly appears as a dominant forcing for Martian cloudiness. Clouds preferentially evolve in the "cold zones" delimited by polar vortex boundaries (polar hoods) or by the intertropical cold and wet region of aphelion (cloud belt). The predicted cloud trends compare reasonably well with the observed ones, attesting of a good overall behavior of this cloud scheme. On the other hand, the predicted cloud mass of the aphelion belt is significantly larger than that deduced by James et al. (1996) from HST observations (3 pr. µm vs. 1). Their estimation is however based on a crystal radius value of 2 µm whereas 3-5 µm are rather inferred by Clancy et al. (2002). The water ice content suggested by these authors could thus be too low by a factor of 2. As stated by Richardson and Wilson (2002b), we also find that the aphelion cloud belt evolution is primarily driven by the thermal behavior of equatorial regions around aphelion and is much less sensitive to water supply from higher latitudes. A noticeable asymmetry distinguishes the northern and the southern polar hoods. Such a statement was also deduced from observations (Wang et al., 2002). The northern hood is uniformly spread between the seasonal cap edge and the pole and features much larger water ice mass than the southern one which geographical extent remains essentially confined to the cap edge. Although it could be argued that the southern winter hemisphere is much drier than the northern winter hemisphere, a more detailed analysis should be conducted to lighten of a potential dichotomy in dynamical regimes between vortices.

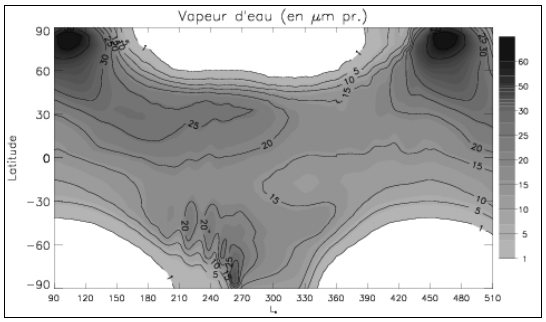

Figure 4: *Same as Fig. 2 but for evolution 1 scheme.*

As illustrated by Figure 4 and Figure 5, the predicted water vapor mass are clearly enhanced when the ability of water ice to be transported is accounted for. Results provided by this cloud scheme compare much better with data than with the basic scheme. Clouds, as a mobile reservoir for water, do not only change the global amount of humidity (by at least a factor of 2), they also change the way water is geographically distributed (Fig. 5: lower graph). According to this graph, this effect is mostly perceptible during northern spring and summer. This change in partitioning water vapor between the northern and southern hemispheres is directly caused by the presence of the aphelion cloud belt. While transferring any supersaturated excess of water vapor to lower layers, the basic scheme unrealistically enhances water confinement.

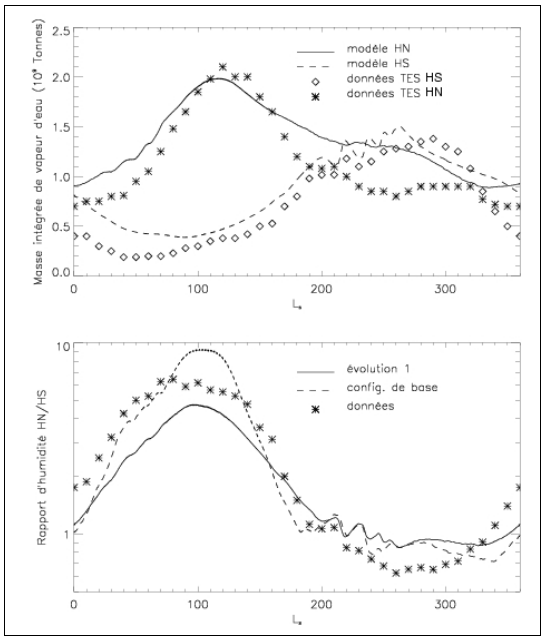

Figure 5: *(Upper graph) Hemispheric integrated water vapor mass (in GTon) (Lower graph) North to south ratio of humidity as a function of L_s: comparison between the evolution 1 (solid line), the basic cloud scheme (dashed line) and TES data (stars).*

Around aphelion, this overestimated effect imposes water to be relatively more sequestered in the northern tropics where the ascending branch of the Hadley cell is located. Evolution 1 cloud scheme allows water ice to be kept aloft at heights corresponding to the return branch of the Hadley cell. The ability of water ice to be transported over long distances is questionable given the influence of water ice particle sedimentation upon it. On the other hand, clouds within the belt are submitted to a strong diurnal thermal cycle. The subsequent amount of water vapor subliming out ice crystals is more efficiently blown southward by winds than the corresponding amount of water ice formed at night. The significant difference in predicted north to south humidity ratio between the two cloud schemes gives a strong theoretical support to the influence of the aphelion cloud belt on the water flux between poles (Clancy et al., 1996). Figure 6 provides a more detailed assessment of the change in geographic distribution of water due to cloud transport. Even though both of our cloud models fail at reproducing the observed mean poleward gradient of water in the southern hemisphere, it can be seen that clouds amplify water vapor abundances

in mid-latitude regions, this result being in very good agreement with observations. This water concentration is done at the high latitude expense. The reason for such a cloud effect on the water cycle is given in Figure 7. This graph indicates that most of water vapor enrichment resulting from cloud transport is realized during northern fall and winter when both hemispheres are partially covered by the CO_2 seasonal deposit (the biggest "black" portion of the graph).

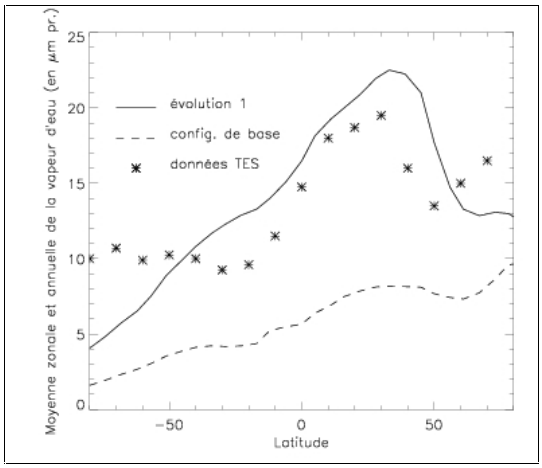

Figure 6: *Zonal and annual averages of the water vapor abundances as a function of latitude, same line styles as in fig. 5.*

At this season, the presence of mid-latitudes baroclinic instabilities assures a strong horizontal mixing organized in a succession of hot and wet fronts pushing poleward while cold and dry fronts are moving equatorward. This redistribution of wet air masses is responsible for a water ice frost deposit theoretically growing thicker at the edge of seasonal caps as the season proceeds. This cold trapped water ultimately returns to poles at the end of the cap recession according to a quasi-solid transport mechanism (Richardson and Wilson, 2002). When cloud transport is accounted for, part of the nebulosity forming above the edge of the seasonal cap can be carried back to mid-latitudes, following cold front trajectories. Clouds blown off the seasonal cap may then release water vapor in the warmer tropical regions. According to the expected circulation regime at this season, water vapor subliming out these detached "polar hood" clouds is then spread within the intertropical region by the lower southward branch of the Hadley cell in a similar way as the cross-equatorial advection of dust storms forming in the northern mid latitudes (Wang, 2002). The likeliness of condensate hazes detaching from the polar hood is supported by Viking Lander data analysis (Tillman, 1979) and by groundbased observations (Akabane, 1995). When the assumption is made that cloud transport is not significant (basic scheme), the predicted water amounts carried by cold fronts is weaker since cold trapping above the cap edge is much more effective in this case.

Conclusion:

The "wet" exchange between the polar hood and the mid latitudes provides a powerful mechanism counteracting the "quasi-solid" return flow of water towards the NPC.

In a sense, clouds can be seen as a humidifying agent of the Martian atmosphere since they allow a greater amount of water to be extracted from the NPC (an effect that is not detailed in the paper) while forcing water to be more concentrated in mid latitude regions during fall and winter seasons, the latter effect being realized at the expense of the CPN.

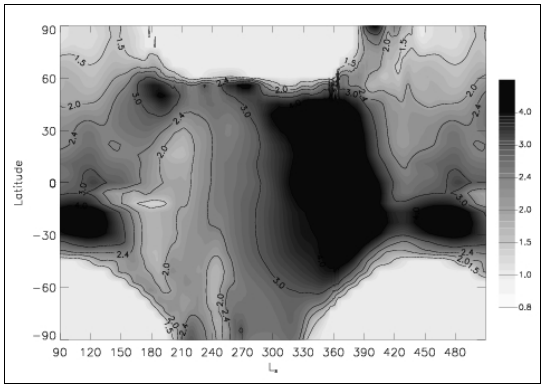

Figure 7: *"Evolution 1" to "basic scheme" ratio of water vapor abundance.*

Bibliography

Akabane, et al., *Aston. Astrophys.* 304, 595-601, 1995.

Bass, D.S., and D.A. Paige, *Icarus*, 144, 397-409, 2000.

Christensen, et al., *JGR* 89, 4587-4596, 1984.

Clancy, R. T., et al., *Icarus* 122, 36-62, 1996.

Clancy, R. T., et al., 2002.

Forget, F., et al., *JGR* 104, 24155-24176, 1999.

Haberle, R.M., and B.M. Jakosky, *JGR* 95, 1423-1437, 1990.

Houben, H., et al., *JGR* 102, 9069-9083, 1997.

Jakosky, B.M, *Icarus* 55, 19-39, 1983.

James, P. B., et al., *JGR* 101, 18883-18890, 1996.

Michelangeli, et al., *Icarus* 100, 261-285, 1993.

Richardson, M.I. and R.J. Wilson, *JGR* 107, 10.1029/2001JE001536, 2002a.

Richardson, M. I. and R.J. Wilson, *JGR*, in press,, 2002b.

Smith, M. D., *JGR* 107, 10.1029/2001JE001522, 2002.

Tillman, et al, *JGR* 84, 2947-2955, 1979.

Wang, H., and A.P. Ingersoll, submitted to *JGR*, 2002.